

# An experimental investigation of the reduced frequency effects into pressure coefficients of a plunging airfoil

M. Mani<sup>1</sup>, F. Ajalli<sup>2</sup> & M. R. Soltani<sup>3</sup>

<sup>1</sup>*Department of Aerospace Engineering,  
Amirkabir University of Technology, Iran*

<sup>2</sup>*Aerospace Research Institute, Iran*

<sup>3</sup>*Department of Aerospace Engineering,  
Sharif University of Technology, Iran*

## Abstract

Aerodynamic coefficients on a two dimensional plunging airfoil, in a low-speed wind tunnel are presented. Dynamic motion was produced by plunging the model over a range of reduced frequencies, and mean angles of attack. The Reynolds number in the present test was held fixed ( $Re = 1.5 \times 10^5$ ), and the reduced frequency was varied in an almost wide range. Surface static pressure distribution was measured on the upper and lower sides of the model, during the oscillating motion. It was found that reduced frequency had strong effects on the pressure distribution, near the leading edge of the airfoil. For mean equivalent angles of attack of 0, 5 degrees, hysteresis loops on the upper surface of the airfoil near the leading edge were counter clockwise and for high mean equivalent angle they were clockwise. By increasing the reduced frequency the hysteresis loops became wider and larger.

*Keywords: unsteady aerodynamic, hysteresis loops, plunging airfoil, reduced frequency.*

## 1 Introduction

In many engineering applications, lifting surfaces experience unsteady motions or are perturbed by unsteady incoming flows. High level dynamic loading and noise generation are inherent problems, due to unsteadiness [1]. One of the basic



problems of flight dynamics is the formulation of the aerodynamic forces and moments acting on a body in an arbitrary motion. For many years the aerodynamic functions were approximated by linear expressions leading to a concept of stability and control derivation but the addition of nonlinear terms are very important and should not be omitted in the control fields. These considerations were many time questioned base on the studies of aerodynamics, which go back to the twenties. Dynamic stall phenomenon appears on helicopters rotor blades, rapidly maneuvering aircraft, wind turbine and even insect wings. In many cases dynamic stall becomes the primary limiting factor in the performance of the associated vehicle or structure [2]. The mechanism of dynamic stall was first identified on helicopters. The importance of unsteady aerodynamics was considered by Harris and Pruyen [3] when helicopter designs were unable to predict the performance of high speed helicopters using conventional aerodynamics. Ham and Garelick [4] observed the extra lift due to vortex formation on the airfoil during the unsteady motion. Carta [5] was able to identify a pressure field on oscillating, two dimensional airfoils that was indicative of the passage of the vortex. Dynamic stall was then explored by McCroskey and Fisher [6] on a model of a rotor. Many of the aerodynamic phenomena governing the behavior of wind turbine blades and helicopter rotors are known, but the details of the flow are still poorly understood and need to be predicted accurately. As a result of this inaccuracy the actual loading are under predicted [7]. Due to the complicated behavior of unsteady forces during the plunging motion, numerical techniques are not able to predict accurately these variables yet, and relatively little experimental information is available about the precise fluid physics of oscillating airfoils. Also pure plunging airfoil motion has received relatively less attention than pitching motion. Therefore the main purpose of this experimental work is to study the pressure distributions at various locations of the Eppler-361 airfoil undergoing sinusoidal plunging oscillation at several angles of attack and different reduced frequencies. Fourteen pressure transducers and the on-line data acquisition system have significantly facilitated the study of the pressure distribution in the plunging airfoil.

## 2 Experimental facility and data processing

All experiments were performed in the subsonic wind tunnel of Amirkabir University of Technology, Department of Aerospace Engineering. The wind tunnel is closed return type, and has a test section of approximately 45 cm wide, 45 cm high, and 120cm long. The Maximum flow speed in the test section of this tunnel is approximately 45 m/s. The inlet of the tunnel has a 7.3:1 contraction ratio with four, anti-turbulence screens and honeycomb in settling chamber to reduced tunnel turbulence to less than 0.1% the test section at all speeds. The airfoil used in this study has an E-361 profile. A 15 cm constant chord airfoil model was designed and manufactured for the test program. To achieve two dimensionality of the flow, the airfoil span has been chosen the same size as the width of the tunnel. Figure 1 shows the airfoil section along with the 14 pressure taps located on upper and lower surfaces used for static pressure measurements.



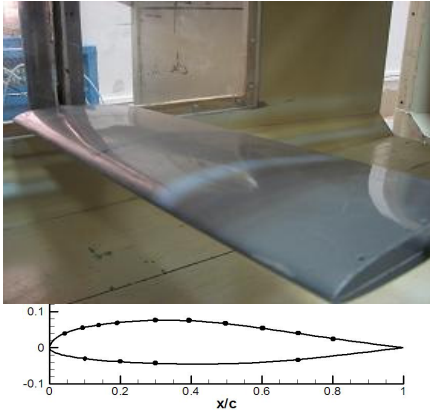


Figure 1: Airfoil section and location of pressure taps.



Figure 2: Oscillation mechanism.

Data are obtained by using differential pressure transducers with a quoted accuracy of 0.2% of full-scale pressure range. Due to the size of selected pressure transducers, we could not place the transducers inside the model. Therefore, the connections between pressure taps and Pressure Transducers are made by tubes. Extensive experiments were conducted to ensure that the time taken for the pressure to reach the transducers is much less than the frequency response of the transducers themselves [8]. The data was processed by using analog to digital board. Oscillatory data were then digitally filtered using various cut-off and transition frequencies to find the best frequencies to fit the original data. The filtering process is necessary to eliminate the electrical noise from the genuine data. The driving mechanism of the plunging airfoil has a simple and versatile design which consists of motor, gears, cam, and shaft. This mechanism can provide various frequencies ( $f$ ), amplitudes ( $h$ ) and mean angles of attack ( $\alpha_0$ ). The motor and gear combination develop a wide range of frequencies. The maximum frequency is 3 Hz. Figure 2 shows the picture of oscillation mechanism.

### 3 Results and discussions

Both static and oscillatory test were conducted at  $Re = 1.5 \times 10^5$ , ( $U_\infty = 15m/s$ ). The instantaneous displacement of the model was measured using a potentiometer. The static pressures at angles of attack 0, 2, 5, 10, 12, 15, 17 and 20 were measured. The surface pressure distribution at mean angles of attack (0, 5, 10 degrees) and different reduced frequencies for constant amplitude of oscillation  $\tilde{h} = 8cm$  are presented in this paper. The effects of the amplitudes of oscillations on the static pressure distribution in dynamic motion are presented in [9].



Figure 3 shows the sinusoidal variation of displacement with non-dimensional time. Relative motions between pitching and plunging airfoils are compared by equivalent angle of attack [10]. The phase difference between two motions is 90degrees (Figures 3 and 4). The height of oscillation and its equivalent angle of attack are defined as:

$$h = \tilde{h} \sin(\omega t)$$

$$\alpha_{eq} = \tan^{-1} \left( \frac{\dot{h}}{U_{\infty}} \right) = k \bar{h} \cos(\omega t)$$

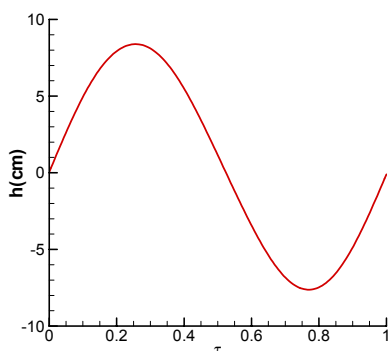


Figure 3: Sinusoidal variations of displacement ( $\alpha_0 = 0$ ).

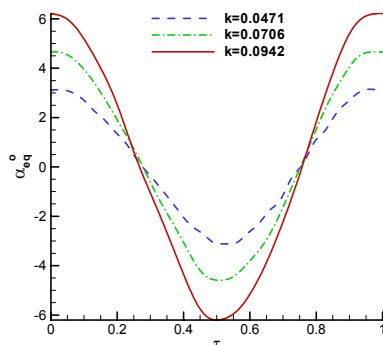


Figure 4: Variations of equivalent angle of attack vs.  $\tau$  ( $\alpha_0 = 0$ ).

There is a crossover point at which the value of pressure in upstroke and down stroke is the same, for specific angle of attack. For example as shown in (fig 5c) at  $k=0.0706$  this angle is 1.8 degrees. By increasing the reduced frequency up to  $k=0.0942$ , the related equivalent angle to crossover point of the "8" shape is decreased to 1.4 degrees which shows an earlier separation of the flow in high frequencies. As mentioned before, the more the reduced frequency, the larger the variation ranges of equivalent angle of attack.

For example at  $\alpha_{mean} = 0$  deg and  $k = 0.0942$ , the equivalent angle of attack is varied over the range of  $(-5.8^\circ < \alpha_{eq} < 5.8^\circ)$ , that have noticeable effects in unsteady behavior of the flow. For the lower surface the direction of the hysteresis loops are clockwise (opposite direction of the upper surface), figure 5d. Variations of  $C_p$  vs.  $\alpha$  in figure 5, shows that the hysteresis loops are larger and widen as reduced frequency increases from  $k=0.0471$  to  $k=0.0942$ , because this parameter ( $k$ ) make the flow more unsteady and reinforce the lag effects of the flow. In this figure, it is observed that, the maximum pressure suction

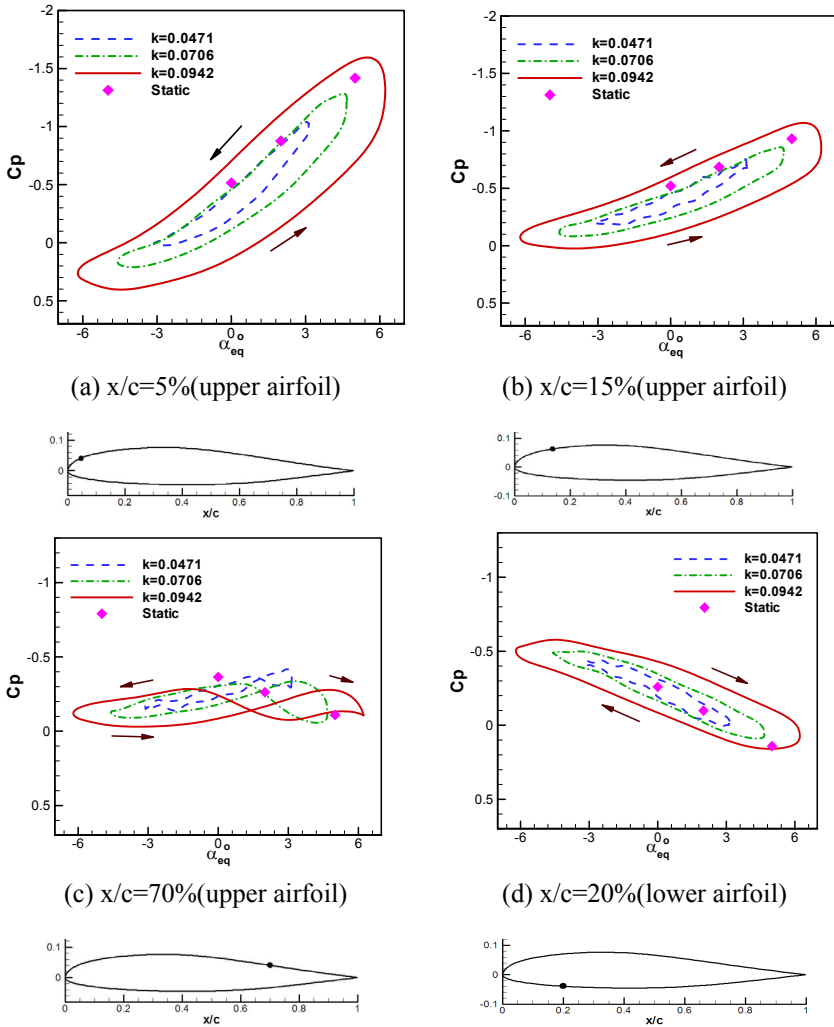


Figure 5: Dynamic variation of the pressure coefficients for  $\alpha_{\text{mean}}=0$  deg.

$|C_p|_{\text{max}} = 1.7$  is near the leading edge at  $x/c=5\%$  of the upper surface and occurs at an equivalent angle of attack about 5.5 degrees for  $k=0.0942$ . One could expect that the maximum pressure suction for  $k=0.0942$  happens at maximum equivalent angle of attack (5.8 degrees), but it happens at  $\alpha_{eq} = 5.5^\circ$ . This is due to the lag effects and delay time of the flow in unsteady motions. At lower value of reduced frequency (for example  $k=0.0471$ ) the delay time of the maximum pressure suction near the leading edge is negligible but it is much significant at higher reduced frequency (fig 5a). At the aft portions of the airfoil the dynamic variations of the pressure coefficient are lower regard to the forward portion.

This indicates that oscillation of the airfoil has no significant effect on the rear portion.

Figure 6 show the variation of pressure coefficients at several ports ( $x/c=5, 15, 60$  and  $70\%$ ) on the upper surface of the airfoil for  $\alpha_{mean} = 5 \text{ deg}$ , meaning that the model was set to an angle of attack of 5 degrees and oscillated at amplitude of  $\pm 8 \text{ cm}$ . In this case, the suction pressure peak near the leading edges at  $x/c=5\%$  and  $x/c=15\%$  are increased. The maximum pressure peak at  $x/c=5\%$  for  $k=0.0942$  in comparison with figure (5a) is increased about  $|\Delta C_p| = 0.8$ . The direction of the hysteresis loops at the positions near the leading edge remains

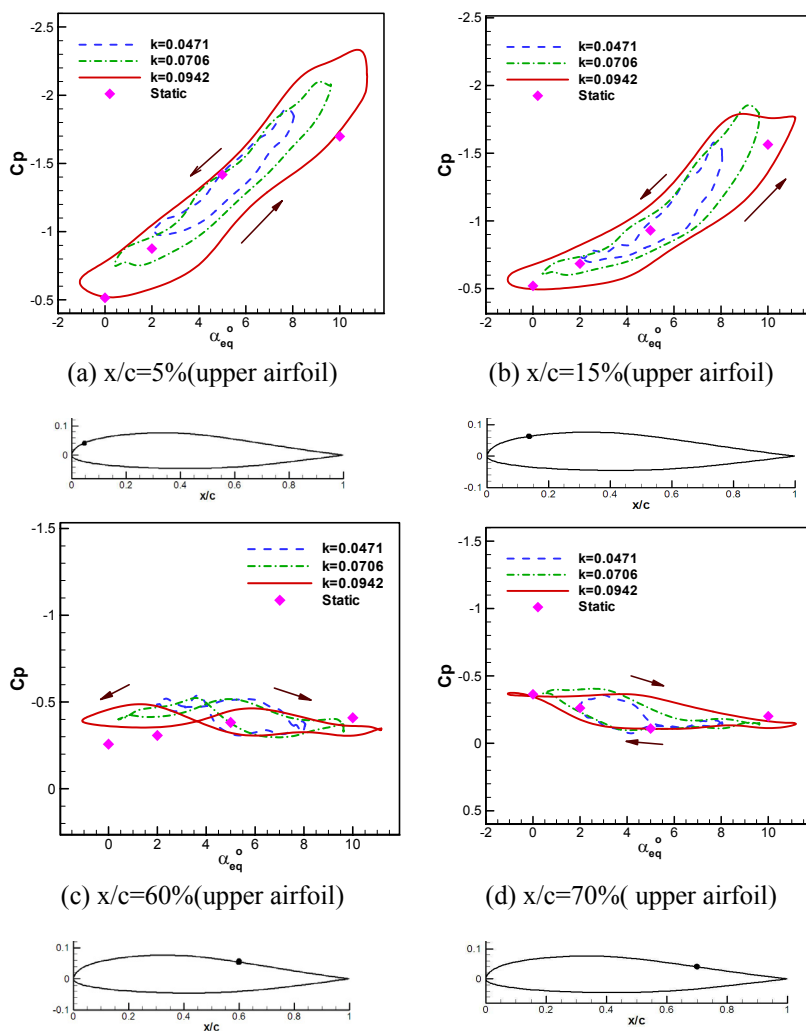


Figure 6: Dynamic variation of the pressure coefficients for  $\alpha_{mean}=5 \text{ deg}$ .



counter clockwise, that indicates the flow is attached yet, but at the aft portion  $x/c=60\%$ , hysteresis loops become like "figure 8" shape which shows the separation has occurred in this position. In the pressure port  $x/c=70\%$ , the direction of the hysteresis loops change to clockwise direction which is caused by the adverse pressure gradient near the trailing edge of the airfoil. Comparison the figures (5c, 6c), showed that the separation of the flow moved forward and happened at  $x/c=60\%$ , because the model was oscillated at higher mean angle of attack. The effects of reduced frequency in this case are observed to be the same as the previous case.

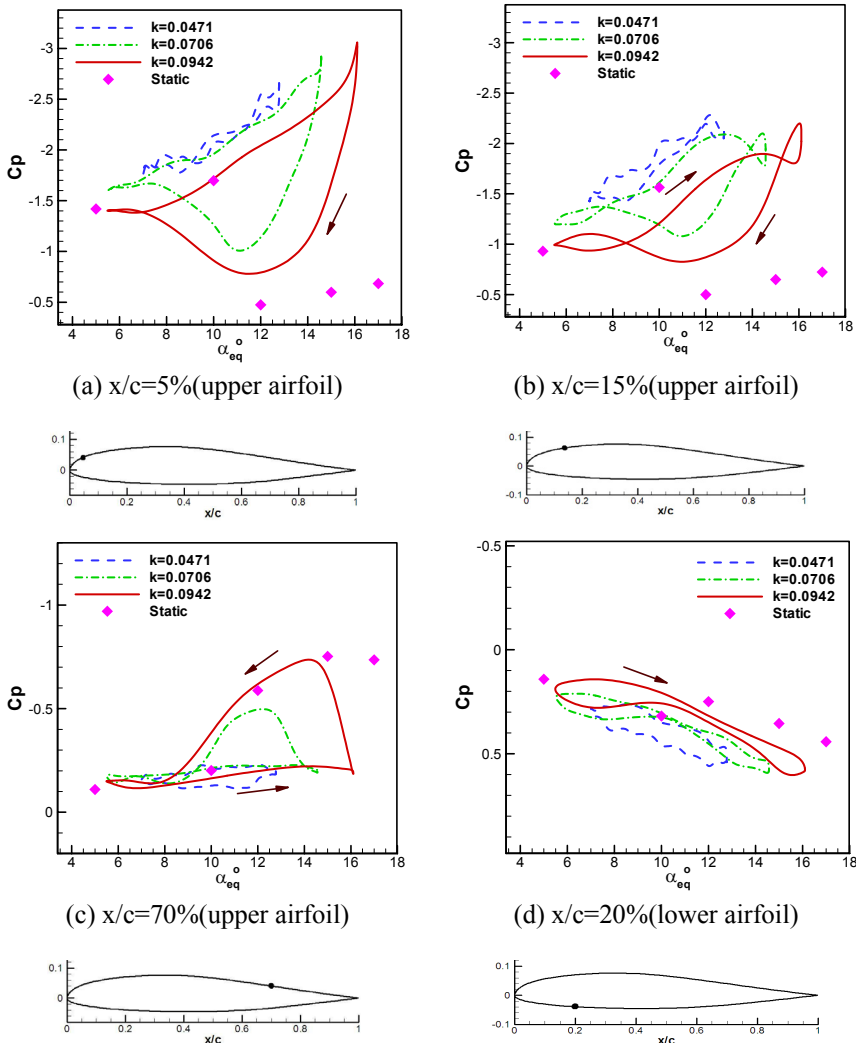


Figure 7: Dynamic variation of the pressure coefficients for  $\alpha_{\text{mean}}=10$  deg.

Figure 7 shows variations of  $C_p$  at higher mean angle of attack, (near static stall angle). Note that the static stall angle for this airfoil occurred at 12 degrees. The directions of hysteresis loops at  $x/c=5\%$  for the upper surface are clockwise which define that the motion has lead phase, figure 7a. When the mean angle of attack is increased up to 10 degrees, the width of the hysteresis loops in this pressure port increase drastically and also the maximum pressure suction is increased for the highest value.

For example the value of maximum pressure in figure (7a) for  $k=0.0942$ , is increased about  $|\Delta C_p|=1.4$  compared to figure 5a. It is observed that after the maximum suction a sudden undershoot of pressure coefficient happened which shows that dynamic starting vortex near the leading edge forms. This starting vortex as obvious in figure 7a, for  $k=0.0706$  happens at  $\alpha_{eq}=16^\circ$  and for  $k=0.0942$  it occurred at  $\alpha_{eq}=14^\circ$ . The speed of starting vortex on the upper surface of the airfoil increases when the reduced frequency is increased.

When the plunging airfoil passes the static stall angle flow reverses near the surface at the rear part of the airfoil. By increasing equivalent angle of attack this reversal flow progresses up the leading edge of the airfoil; then at an angle of attack that depend on many parameters including frequency, airfoil shape, Reynolds number etc, the viscous flow no longer remains thin and attached, and a very strong vertical flow develops.

This vortex being near the leading edge of the airfoil, enlarges, and then moves down the airfoil then produces the phenomena known as dynamic stall. The vortex shedding process is the most obvious characteristic of dynamic stall [2]. In this case ( $\alpha_{mean}=10^\circ$ ), the variations range of the equivalent angle of attack was not enough large to cause deep stall and light stall [12] happened. In position  $x/c=15\%$ , three hysteresis loops are formed which the largest one is clockwise and lead phase. The maximum overshoot in figure 7c, ( $x/c=70\%$  upper surface), shows the progressing of the starting vortex to trailing edge of the airfoil. Further from figure 7 note that, at the lower reduced frequency  $k=0.0471$ , there is no indication of the sudden undershoot and progressing of the starting vortex in the airfoil. On the lower surface, figures 7d, the directions of the hysteresis loops are clockwise. There is a lower pressure variations on the lower surface compared to the upper surface which is due to the shape of the airfoil. Hysteresis loops on the lower surface in this case in comparison with the figure 5d ( $\alpha_{mean}=0^\circ$ ), become narrower.

## 4 Conclusion

An extensive experimental study was conducted to investigate the flow phenomena over the plunging airfoil. Static pressure distributions at 14 positions over and under the model were measured. At mean angles of attack 0, 5 deg, hysteresis loops in forward portion of the airfoil were counter clockwise and the flow was attached. Near the trailing edge of the airfoil where the flow was separated, hysteresis loops formed an "8" shape and at lower surface hysteresis





loops were clockwise. The directions of hysteresis loops for  $x/c=5\%$  and  $\alpha_{\text{mean}}=10\text{deg}$  on the upper surface were clockwise and the dynamic starting vortex was formed. The higher reduced frequency resulted larger hysteresis loop which was due to strong effects of unsteadiness. There was a lower pressure variations on the lower surface compared to the upper surface of the airfoil. In the aft portions of the airfoil the dynamic variations of the pressure coefficient were less regard to the forward portion.

## References

- [1] McCroskey, W. J., *Recent Developments in Dynamic Stall*, Symposium on Unsteady Aerodynamics, Vol. 1, Univ. of Arizona, March 1975, pp. 1–34
- [2] Carr L. W., *Progress in Analysis and Prediction of Dynamic Stall*, Journal of Aircraft, Vol. 25, No.1, January 1988.
- [3] Harris, F. D. and Pruyn, R. R., *Blade Stall-Half Fact, Half Fiction*, Journal of American Helicopter Society, Vol. 13, No. 2, April 1968, pp. 27-48.
- [4] Ham, N. D. and Garelick, M. S., *Dynamic Stall Considerations in Helicopter Rotors*, Journal of American Helicopter Society, Vol.13, No.2, April 1968, pp. 49–55.
- [5] Carta, F.O., *Experimental Investigation of the Unsteady Aerodynamic Characteristics of a NACA 0012 Airfoil*, Res.Rep. M-1283-1, United Aircraft Corp., July 1960.
- [6] McCroskey, W. J., Fisher, R. K., *Detailed Aerodynamic Measurements on a Model Rotor in the Blade Stall Regime*, Journal of American Helicopter Society, Vol.17, No.1, Jan. 1972, pp. 20–30.
- [7] Johansen, J. *Prediction of Laminar/Turbulent Transition in Airfoil flows*, Riso-R-987 (EN), Riso National Laboratory 1977.
- [8] Mani, M., Soltani M. R. and Tolouei E., *An Experimental Study of Time Lag Pressure Measurement in Different Tubes*, Amirkabir, Vol.16, No.61-B, Spring 2005.
- [9] Ajalli F., Mani M., Soltani M. *An Experimental Investigation of Pressure Distribution around a Heaving Airfoil*, The 5<sup>th</sup> International conference on Heat Transfer, Fluid Mechanics and Thermodynamics, South Africa, Spring 2007.
- [10] Carta, F.O. *A Comparison of the Pitching and Plunging Response of an Oscillating Airfoil*, NASA CR-3172, 1979.
- [11] Lishman J.Gorden, *Principles of Helicopter Aerodynamics*, Cambridge University Press, 2000.
- [12] McCroskey, W. J., *Unsteady Airfoils*, Annual Report of Fluid Mechanics, Vol. 14, pp. 285–311, 1982.

